Finite-element analysis of electrostatic interactions in electrorheological fluids

R. Tao, Qi Jiang, and H. K. Sim*

Department of Physics, Southern Illinois University, Carbondale, Illinois 62901

The Laplace equation for an infinite chain of dielectric particles in an electrorheological fluid is solved with the finite-element analysis (FEA) method. The FEA results reveal that the dipole model gives a good approximation in calculating energy, even if neighbor particles are very close and the mismatch is moderate. However, the dipole model underestimates the pair attractive force when the particles are in or near contact. On the other hand, the conductor model is a good approximation when the two particles are near contact and the mismatch is very big. Otherwise, the conductor model overestimates the pair attractive force. A formula to calculate the neighbor-pair attractive force for the whole range is proposed. The FEA results agree with this formula reasonably well.

PACS number(s): 82.70.Gg, 61.90.+d, 64.90.+b

I. INTRODUCTION

An electrorheological (ER) fluid consists of fine dielectric particles suspended in a liquid of low dielectric constant [1–5]. Interesting phenomena observed in the ER fluid, such as rapid variation of viscosity and solidification of the fluid, are all induced and controlled by an applied electric field. The reversible ER effect occurs in milliseconds and has a high potential for technological applications.

In recent years, many attempts have been made to provide detailed theoretical descriptions for ER fluids [6–8]. A widely adapted approach is to treat each polarized particle in an ER fluid as a point dipole associated with a hard core [6,7]. This dipole model has some success in explaining and predicting the ER effect. For example, a prediction based on the dipole model that the ground state of an ER fluid is a body-centered tetragonal lattice [7] was experimentally confirmed [9]. Various computer simulations based on the dipole model also produced some good results [10–13].

When the ER fluids have a small dielectric mismatch between the particles and the base liquid, the dipolar approximation may be sufficient. However higher-multipole contributions may be important when the dielectric mismatch is large and the particles are nearly touching [14–19]. The calculation for higher-multipole contributions is not as simple as that for dipoles. Recently, a conduction model was proposed to explain the ER effect under dc or low ac fields [20]. Since this model is quite different from the dipole model, it is important to have knowledge about the following information: Under what condition is the dipolar approximation valid? When is the dipolar approximation not sufficient? Under what condition is the conduction model valid? What is

the complete description of ER fluids? To answer the above questions, we must have some exact numerical solutions to compare with.

When an ER fluid is in an electric field, dielectric particles quickly form chains between two electrodes. A physical chain and its infinite images are equivalent to an infinite chain. Therefore, in this paper, we will solve the Laplace equation for an infinite chain system with the finite-element analysis (FEA) method. Our ER system has spheric dielectric particles of dielectric constant ϵ_p and the liquid of dielectric constant ϵ_f. The results are clearly determined by two parameters, the dielectric mismatch

$$\kappa = \epsilon_p / \epsilon_f , \qquad (1.1)$$

and the distance between two neighbor particles d in the unit of sphere radius a.

A similar problem was studied in Ref. [14] with truncated multipole expansion for a chain of up to 40 particles. Their result indicates that the interaction force and energy between two touching dielectric spheres are divergent, even if the spheres have a finite dielectric constant. This result seems to be artificial because touching dielectric particles in ER fluids do not collapse in reality.

Recently, Anderson also studied this problem and especially examined the situation of a large κ [15]. He found that for a large dielectric mismatch the attractive force between two neighbor particles is proportional to κ^2 when they are in contact.

Our FEA method enables us to solve the system exactly for the whole range of interest. Our calculation covers the whole range from a small κ to a large κ. We will report about the electric field, surface charge distribution, interaction energy, and attractive force as functions of κ and d. Based on our FEA calculation, we have proposed a formula to calculate the pair attractive force. This formula does not only agree with the conductor model and Anderson's result at a very large κ and $d \rightarrow 2a$, but also approaches the dipole model when κ is not very big.

Our paper is organized as follows. In Sec. II, we will

---

*On sabbatical leave from Department of Physics, National University of Singapore, Kent Ridge, Singapore 0511.

define the problem, outline the method, and derive a set of theoretical equations for the system. These equations provide a base for our calculations and clarify what physical quantities we should look for. In Sec. III, we will discuss the dipole model and the conductor sphere model and list the necessary formulas that will be used for comparison. In Sec. IV, we present our results and compare them with the dipole model, the conductor model, and other published results. Finally in Sec. V, we summarize our findings.

II. MODEL AND METHOD OF FINITE DIFFERENCE

As mentioned before, in response to an applied electric field E_0, the dielectric spheres form a chain in the field direction. We assume that the separation between two neighboring spheres is $d = 2D_2$ (Fig. 1). The chain is close packed if $d = 2a$. Our present results are only from the dielectric mismatch model which is valid for ER fluids made of perfectly insulating materials or for ER fluids in a high ac field. However, our method can be easily extended to include cases with nonvanishing conductivity. Then, in the calculation we must use a complex dielectric constant $\epsilon = \epsilon_0 + i4\pi\sigma_0/\omega$, which is related to the dielectric constant ϵ_0, conductivity σ_0, and the field frequency ω.

We take the line passing through the sphere centers as the z axis. The electric potential is given by

$$U = U_0 + \Phi ,$$ (2.1)

where $U_0 = -|E_0|z$ and Φ is produced by the induced bound charges on the sphere surfaces. In the cylindrical coordinate, the Laplace equation is given by

$$\frac{\partial^2\Phi}{\partial\rho^2} + \frac{1}{\rho}\frac{\partial\Phi}{\partial\rho} + \frac{\partial^2\Phi}{\partial z^2} = 0 .$$ (2.2)

U and Φ are functions of ρ and z only. The symmetry provides $\Phi(\rho,z) = -\Phi(\rho,-z)$. We only need to solve the Laplace equation (2.2) for a two-dimensional strip in Fig. 2. Theoretically, D_1 should extend to infinity. We have found in our calculation that as $D_1 \geq 10a$, the solution is almost independent of the values of D_1.
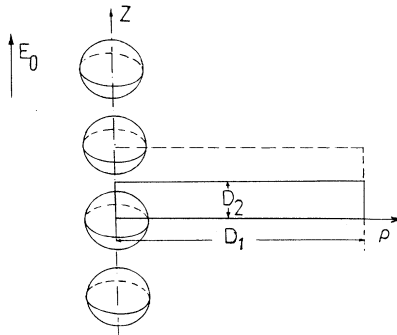

FIG. 1. Infinite chain of spherical ER fluid particles. The rectangular strip, where $D_2 = d/2$ is half the distance between the centers of two neighboring particles and D_1 extends to infinity, is the basic unit for the FEA calculation.
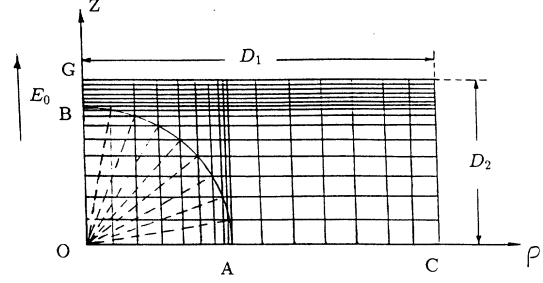

FIG. 2. FEA mesh used for the numerical calculation.

In applying the FEA method, we generate a mesh in Fig. 2 to discretize the Laplace equation. We first divide $\angle LAOB$ evenly into a large number of divisions. Then, at all cross points of the circle and the radii, we draw lines parallel to the z axis and ρ axis. Outside the circle, we further divide $\overline{AC}$ evenly into many divisions. The boundary conditions are given by

$$\Phi(\rho,0) = \Phi(\rho,D_2) = 0, \quad \partial\Phi(0,z)/\partial\rho = 0 ,$$

and $\Phi(D_1,z) = 0 .$ (2.3)

On the sphere surface, U is continuous and

$$\kappa\left[\rho\frac{\partial U}{\partial\rho} + z\frac{\partial U}{\partial z}\right]\Bigg|_{r=a-} = \left[\rho\frac{\partial U}{\partial\rho} + z\frac{\partial U}{\partial z}\right]\Bigg|_{r=a+} ,$$ (2.4)

where $r = \sqrt{\rho^2 + z^2}$.

Since E_0 and hence the applied voltage are maintained as constants, the following electrostatic energy W characterizes the interaction,

$$W = \frac{1}{8\pi}\left[\int E\cdot D\,dr - \int E_0\cdot D_0\,dr\right] ,$$ (2.5)

where $D_0 = \epsilon_f E_0$ and $D = \epsilon(r)E$, with $\epsilon(r) = \epsilon_f$ or ϵ_p according to the region. After the thermal energy is ignored, W should be maximum in the ground state [21]. Rewrite W as

$$W = \frac{1}{8\pi}\left[\int (E - E_0)\cdot(D + D_0)\,dr\right.$$

$$\left. + \int (E_0\cdot D - E\cdot D_0)\,dr\right] .$$ (2.6)

As $E - E_0 = \nabla(U_0 - U)$, the first integral can be shown to vanish by the following transformation:

$$\frac{1}{8\pi}\int dr\{\nabla\cdot[(D + D_0)(U_0 - U)] - (U_0 - U)\nabla\cdot(D + D_0)\} .$$ (2.7)

There is no free charge within the bulk of the system, then $\nabla\cdot(D + D_0) = 0$. The first term in Eq. (2.7) is also vanishing because it can be transformed into a surface integration and $U = U_0$ at the infinity. Then, the interaction energy per particle is given by

$$w = \frac{W}{N} = \frac{(\epsilon_p - \epsilon_f)}{8\pi}\int_{sphere} E_0\cdot E\,dr ,$$ (2.8)

where the integration is taken within a sphere and N is the total number of the spheres in the chain.

The bound charges are only on the sphere surfaces with a density given by

$$
\begin{aligned}
\sigma &= -\frac{(\epsilon_p - \epsilon_f)}{4\pi\epsilon_f} \left[\frac{\partial U}{\partial r} \right] \Bigg|_{r=a-} \\
&= -\frac{(\epsilon_p - \epsilon_f)}{4\pi\epsilon_p} \left[\frac{\partial U}{\partial r} \right] \Bigg|_{r=a+} .
\end{aligned}
\tag{2.9}
$$

Since $\mathbf{E}_0 = -\nabla U_0$ and $\nabla \cdot \mathbf{E} = 0$, we have

$$
\int \mathbf{E}_0 \cdot \mathbf{E} d\mathbf{r} = -\oint_{\text{sphere}} U_0 E_r ds \ ,
\tag{2.10}
$$

where the integration is over a sphere surface. We can transform Eq. (2.8) into a surface integration,

$$
w = -\frac{\epsilon_f}{2} \oint_{\text{sphere}} U_0\,\sigma ds \ .
\tag{2.11}
$$

Since $U_0 = -\mathbf{E}_0 \cdot \mathbf{r}$, we have

$$
w = \tfrac{1}{2}\epsilon_f \mathbf{E}_0 \cdot \mathbf{p} \ ,
\tag{2.12}
$$

where $\mathbf{p} = \oint_{\text{sphere}} \mathbf{r}\sigma\,ds$, the induced dipole moment of the sphere. Therefore, in the preferred state sphere has the strongest dipole moment. When we stretch the chain, the elastic force per particle is given by

$$
f_e = \frac{\partial w}{\partial d} \ .
\tag{2.13}
$$

The induced interaction energy between two dielectric spheres is given by

$$
u_{ij} = \tfrac{1}{2} \int \frac{\sigma_i \sigma_j}{\epsilon_f r_{ij}} ds_i ds_j \ ,
\tag{2.14}
$$

and the force between them is given by

$$
\mathbf{f}_{ij} = \int \frac{\sigma_i \sigma_j \mathbf{r}_{ij}}{\epsilon_f r_{ij}^3} ds_i ds_j \ .
\tag{2.15}
$$

The situation is specially of interest when these two particles i and j are neighbors. However, f_e in Eq. (2.13) is usually different from the neighbor-pair force calculated from Eq. (2.15). For example, as will be shown in next section, f_e in the dipolar model is about 20% higher than the neighbor-pair force. The above formulas clarify what quantities we should look for and provide a basis for our calculation.

III. DIPOLE MODEL AND CONDUCTOR SPHERE MODEL

Under the dipolar approximation, the integration energy between two particles in the chain is given by

$$
u_{ij}^d = -\frac{2p^2}{\epsilon_f d_{ij}^3} \ ,
\tag{3.1}
$$

where the dipole moment $\mathbf{p}$ is given by

$$
\mathbf{p} = \beta a^3 \epsilon_f \mathbf{E}_{\text{loc}} \ ,
\tag{3.2}
$$

where $\beta = (\kappa - 1)/(\kappa + 2)$. The force between two dipoles

in the chain is attractive in the z direction,

$$
f_{ij}^d = -\frac{6p^2}{\epsilon_f d^4} \ ,
\tag{3.3}
$$

where $\mathbf{E}_{\text{loc}}$ is the local field. With a self-consistent method, we can find

$$
\mathbf{E}_{\text{loc}} = \frac{\mathbf{E}_0}{1 - 4\beta a^3 \zeta(3)/d^3} \ ,
\tag{3.4}
$$

where $\zeta(3) = 1 + (\tfrac{1}{2})^3 + (\tfrac{1}{3})^3 + \cdots = 1.202\,06$. Combining Eqs. (3.2) and (3.4) we have the attractive force between two neighbor dipoles,

$$
f_{\text{pair}} = -\frac{6\beta^2 \epsilon_f E_0^2 a^6/d^4}{(1 - 4.8082\beta a^3/d^3)^2} \ .
\tag{3.5}
$$

From Eq. (2.12), under the dipolar approximation,

$$
w = \frac{\epsilon_f}{2}\mathbf{E}_0 \cdot \mathbf{p} = \frac{\epsilon_f a^3 \beta E_0^2}{2(1 - 4.8082\beta a^3/d^3)} \ .
\tag{3.6}
$$

From Eqs. (3.1) and (3.2), the induced interaction between two neighbor dipoles is given by

$$
u = -\frac{2\epsilon_f \beta^2 E_0^2 a^6/d^3}{(1 - 4.8082\beta a^3/d^3)^2} \ .
\tag{3.7}
$$

When we stretch the chain, the elastic force per particle is

$$
f_e = \partial w / \partial d = \zeta(3) f_{\text{pair}} \ .
\tag{3.8}
$$

It is clear that f_e is about 20% stronger than f_{pair}.

Our conductor model has all dielectric particles in the chain replaced by metallic spheres. This model can be realized from the dielectric mismatch model by letting $\kappa = \epsilon_p/\epsilon_f \to \infty$. The electric field is concentrated between two neighbor metallic spheres [22]. The potential difference between the two neighbor spheres is $E_0 d$. As shown in Fig. 3, $A_1 A_2 = d - 2a\cos\theta$. The electric field between A_1 and A_2 is $E_0 d/(d - 2a\cos\theta)$. The electrostatic energy can be estimated by

$$
w = \frac{1}{8\pi} \int_0^{\pi/2} 2\pi a^2/\sin\theta \cos\theta\, d\theta \frac{(E_0 d)^2}{d - 2a\cos\theta} \ .
\tag{3.9}
$$

Equation (3.9) can be evaluated easily,

$$
w = \frac{\epsilon_f E_0^2 d^3}{16} \left[\ln\left[\frac{d}{d - 2a} \right] - \frac{2a}{d} \right] \ .
\tag{3.10}
$$

The attractive force between these neighbor spheres is ap-

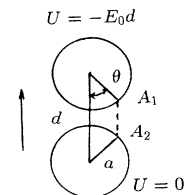

FIG. 3. Region between the two conductor spheres.

proximated by

$$f = -\frac{\epsilon_f E_0^2 d^2}{16} \left[\frac{2a}{d-2a} + \frac{4a}{d} - 3\ln\left[\frac{d}{d-2a} \right] \right] . \quad (3.11)$$

The above result is good only if d is very close to $2a$. Thus, the leading term is given by

$$f \approx -\frac{\epsilon_f E_0^2 a^3}{2(d-2a)} . \quad (3.12)$$

The results from the above two models will be compared with our finite-element calculations.

IV. RESULTS AND DISCUSSIONS

In our calculation, we vary the dielectric mismatch κ from 2 to 50 000 and make the distance d from $2.1a$ approaching $2a$.

A. Electric fields

Figure 4(a) shows the electric potential U at $\kappa=2.5$ and $d=2.1a$, while Fig. 4(b) shows U at $\kappa=2.5$ and $d=2.001a$. In both cases, the electric field inside the sphere is quite uniform, clearly indicating that the dipolar approximation is quite good at $\kappa=2.5$, even if the two
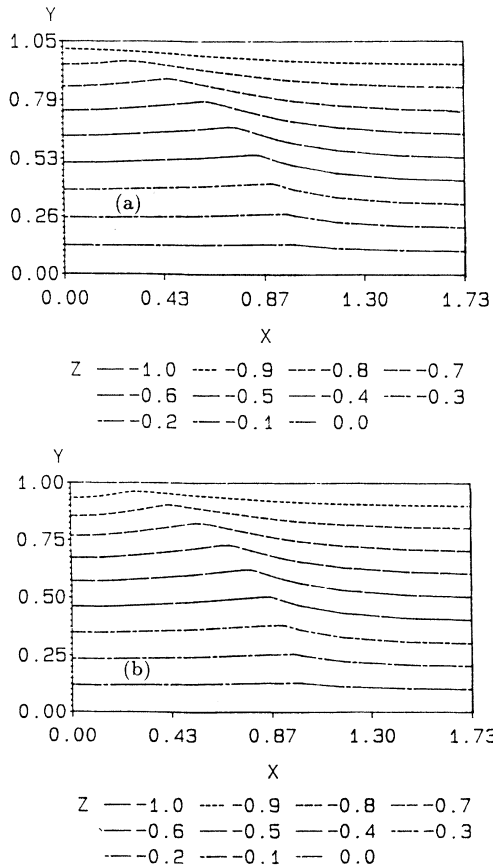

FIG. 4. Electric potential U (in units of E_0a). (a) $\kappa=2.5$ and $d=2.1a$. (b) $\kappa=2.5$ and $d=2.0001a$.
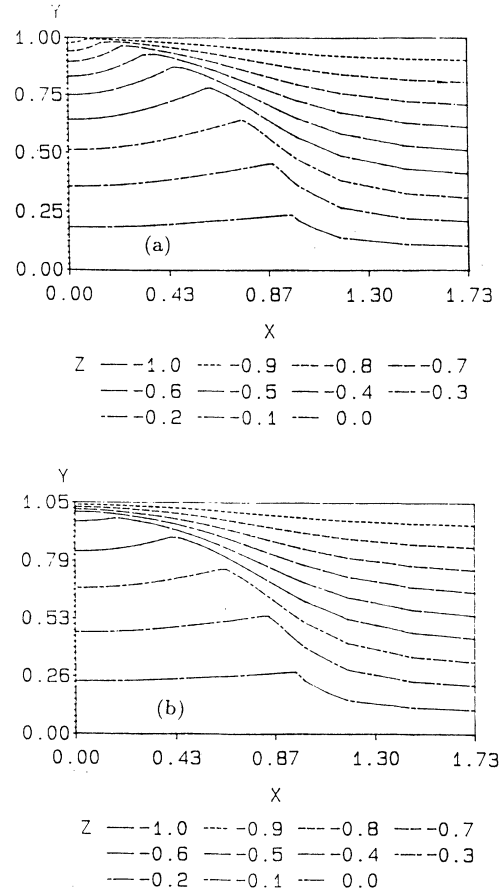

FIG. 5. Electric potential U (in units of E_0a). $\kappa=10$ and $d=2.1a$. (b) $\kappa=10$ and $d=2.0001a$.

spheres are very close.

When $\kappa=10$, the electric field at $d=2.1a$ is still not too far from the dipolar approximation [Fig. 5(a)]. However, at $d=2.0001a$ [Fig. 5(b)], the field is different from the dipolar approximation because the field inside the sphere is no longer uniform. From the above electric potential, we can easily calculate the electric field. For example, at $d=2.0001a$, the electric field near the polar region is much stronger than the dipolar approximation. Our field is stronger than the previous result obtained by the multipole expansion [14].

When $\kappa=5000$, the electric field is quite different from the dipolar model. Figures 6(a) and 6(b) show the case $d=2.1a$ and the case $d=2.0001a$, respectively. A comparison of these two figures clearly shows that as the spheres get closer, the electric field is more concentrated between the two spheres. In addition, the electric potential inside the sphere is almost a constant, which indicates that the conductor sphere model may be good for this situation.

To examine the detail of the electric field, in Fig. 7 we plot U right outside the sphere surface as a function of angle θ for $\kappa=50000$, and $d=2.0002a$, $d=2.002a$, $d=2.02a$, and $d=2.2a$, respectively. It is clear that at $\kappa=50\,000$, the dielectric particles are close to conductor
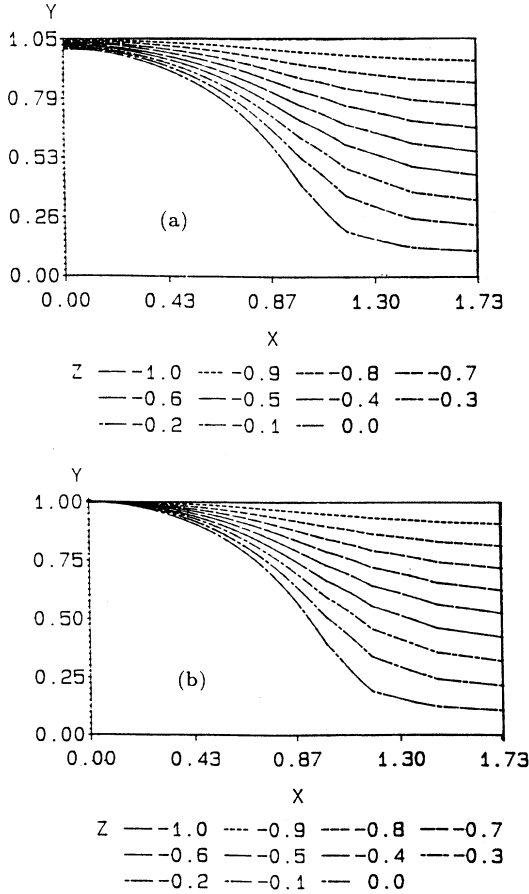
FIG. 6. Electric potential U (in units of E_0a). (a) $\kappa = 5000$ and $d = 2.1a$. (b) $\kappa = 5000$ and $d = 2.0001a$.
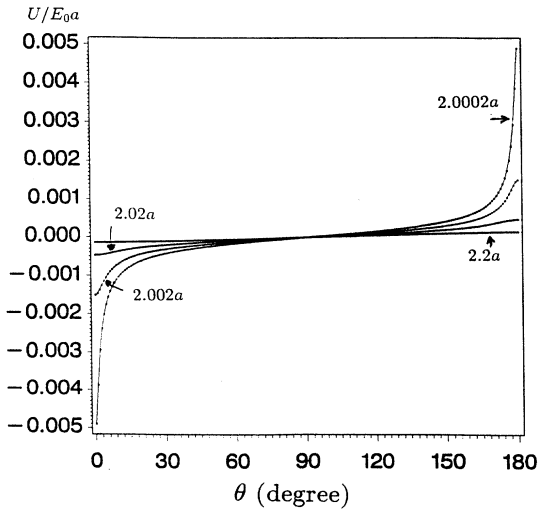

FIG. 7. Electric potential U (in units of E_0a) on the sphere surface vs θ at ($\kappa = 50\,000$) for $d = 2.0002a$, $2.002a$, $2.02a$, and $2.2a$.
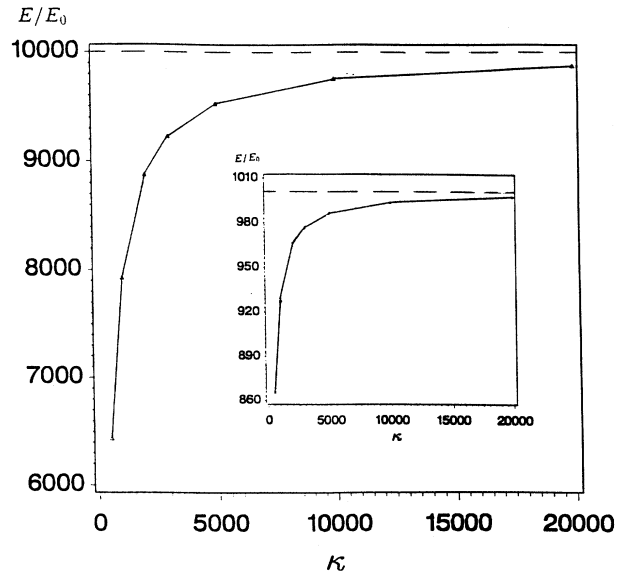

FIG. 8. Electric field at the pole on the sphere surface at $d = 2.0002a$ vs κ. The inset shows the same physical quantity at $d = 2.002a$. $-\,-\,-$, results of the conductor model; $\triangle$ points, FEA results.

particles. Indeed, U only deviates from zero near $\theta = 0$ or π where the surface charge is concentrated. In the case $d = 2.2a$, U is almost zero on the whole surface, $|U/(E_0a)| \leq 5 \times 10^{-3}$, indicating very low surface charge density. As d is reducing, the electric field gets stronger in the polar region.

Since the electric field near the polar region is most sensitive to κ and the distance d, in Fig. 8 we plot the electric field on the sphere surface right at the pole $\theta = 0$ as a function of κ at $d = 2.0002a$ and $d = 2.002a$. All FEA results can be divided into two regions: a transition region and a plateau. In the transition region, the electric field increases quickly with κ. The previous calculation found plateaus at $\kappa \approx 50$ [14]. Our results indicate that the plateau depends on the d. For example, when $d = 2.0002a$, the field continues to increase, even if $\kappa \approx 5000$. In the flat region, the electric field approaches to a constant. For a comparison, in Fig. 8 we also plot two dashed horizontal lines, which are the results of the conductor model at the aforementioned distances, $E_0d/(d-2a)$. The similarity of the two curves in Fig. 8 indicates that there is a scaling relationship, $E = g(\kappa)E_0d/(d-2a)$, where $g(\kappa)$ is a function of κ only.

In order to have a further comparison with the dipolar model at low κ, we plot the induced surface charge density σ at $\kappa = 2$ and $d = 2.02a$ in Fig. 9(a). To examine σ, we expand it in terms of Legendre polynomials,

$$\sigma(\theta) = \sum_l c_l P_l(\cos\theta) \,. \tag{4.1}$$

Because $\sigma(\theta) = -\sigma(\pi - \theta)$, $c_l = 0$ for all even l. Nonvanishing coefficients are listed in Table I. We note that the
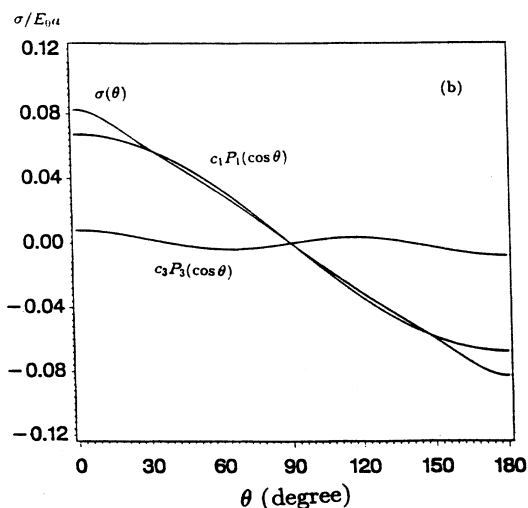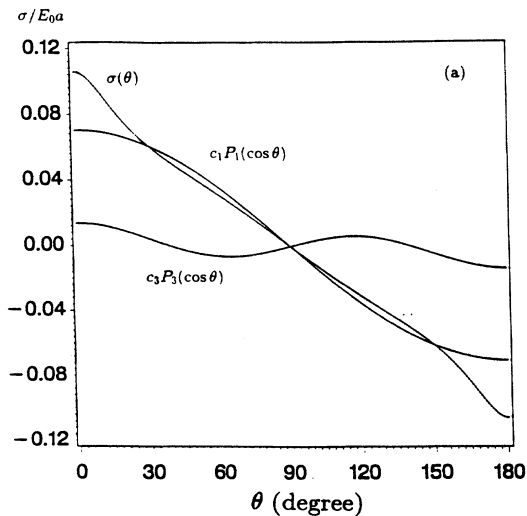
FIG. 9. Surface charge density σ (in units of $E_0 a$) vs θ, the leading term in its expansion $c_1 P_1$ ($\cos\theta$), and the second term $c_3 P_3(\cos\theta)$. (a) $\kappa = 2$ and $d = 2.02a$. (b) $\kappa = 2$ and $d = 2.2a$.

dipole model would be exact if $c_l = 0$ for $l \geq 2$. Table I shows, for example, at $d = 2.02a$ and $\kappa = 2$, $c_3 / c_1 \sim 19.5\%$. The dominance of c_1 implies that the dipole model is a good approximation when κ is not very big. In Table I we also list the coefficients for the same κ at $d = 2.2a$, where $c_3 / c_1 \sim 11\%$. The corresponding sur-

TABLE I. Coefficients in the series expansion of surface charge density for $\kappa = 2$.

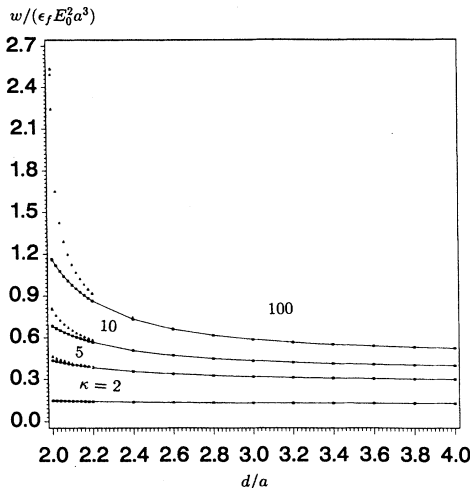| Coefficient	d	2.02a	2.2a
c_1		0.0703	0.0674
c_3		0.0137	0.0080
c_5		0.0095	0.0044
c_7		0.0053	0.0017
c_9		0.0029	0.0007
c_{11}		0.0016	0.0002

FIG. 10. Electrostatic energy per particle w (in units of $\epsilon_f E_0^2 a^2$) vs d for $\kappa = 2$, 5, 10, and 100, respectively. The curves are from the dipolar approximation.

face charge shown in Fig. 9(b) is clearly even closer to $c_1 \cos\theta$ than that in Fig. 9(a). Therefore, the dipole model provides an even better approximation if the distance d increases slightly.

B. Interaction energy

Figure 10 presents the interaction energy per particle, w, as a function of spacing d at $\kappa = 2$, 5, 10, and 100, respectively. The maximum value of w is reached when d approaches $2a$. The curves in Fig. 10 are the results from the dipolar model in Eq. (3.6). It is clear that the dipolar approximation is quite good for $\kappa \leq 10$. At $\kappa = 2$, there is almost no difference in the energy between the FEA re-
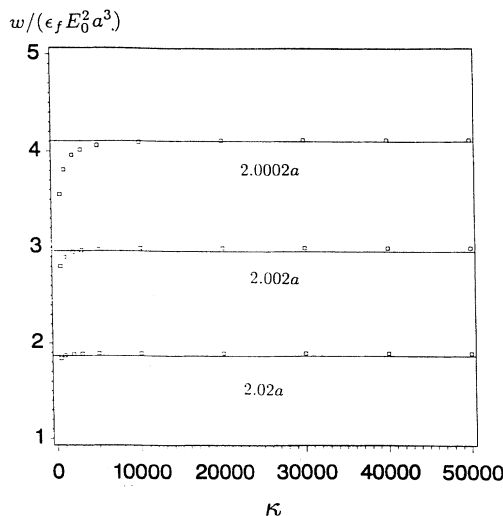

FIG. 11. Electrostatic energy per particle w (in units of $\epsilon_f E_0^2 a^3$) vs κ for $d = 2.0002a$, 2.002a, and 2.02a, respectively. The three horizontal lines are the results from the conductor model.
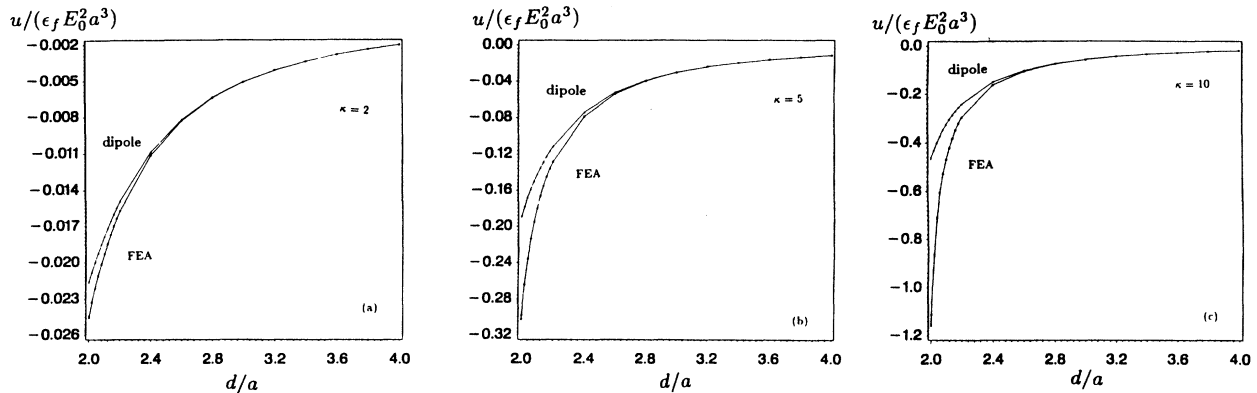
FIG. 12. Pair interaction energy between two neighbor spheres vs the distance d. (a) $\kappa=2$, (b) $\kappa=5$, and (c) $\kappa=10$. The results from the dipole model are included for comparison.

sult and the dipolar approximation. At $\kappa=10$ and $d=2a$, the dipolar model only differs from the FEA results by 15%. However, at $\kappa=100$ and $d=2a$, the difference between the FEA calculation and the dipole model is quite big.

In Fig. 11 we plot w vs κ at $d=2.02a$, 2.002a, and 2.0002a. The three horizontal lines are the results of the conductor model in Eq. (3.10). As κ increases, w approaches a plateau. However, it is clear from Fig. 11 that Eq. (3.10) underestimates w at $d=2.02a$ and $d=2.002a$. The situation is improved at $d=2.0002a$. This is easy to understand because Eq. (3.10) only considers the electric field between two neighbor spheres, and only as $d\rightarrow2a$ is this approximation good.

We also calculated the pair interaction energy between two neighbor particles from Eq. (2.14). In Figs. 12(a)–12(c), we plot the pair interaction energy from the FEA result and from the dipole approximation at $\kappa=2$, 5, and 10, respectively. It is clear again that when $\kappa\leq10$,

the pair energy obtained with the FEA method is very close to the results of the dipole model, even if the two particles are nearly contacting each other.

C. Attracting force

Figures 13(a)–13(c) illustrate the neighboring attractive force vs distance d between two neighboring spheres at $\kappa=2$, 5, and 10, respectively. We apply Eq. (2.15) in our calculation. The result from the dipole model, Eq. (3.5), is also plotted in Fig. 13 for comparison. The above results again indicate that the dipole model provides a reasonably good approximation if κ is not very big. The deviation from the dipole model comes when the spheres begin to contact. The FEA calculation shows that the attractive force between two touching dielectric spheres is stronger than the result from the dipole model when two spheres contact each other. In addition, the higher κ is, the stronger the attractive force is. For example, at
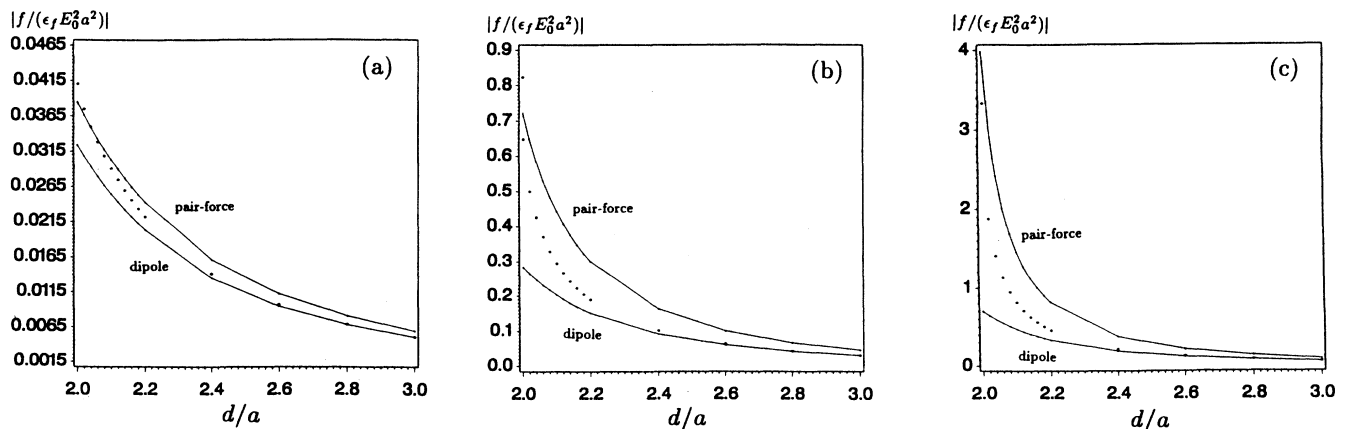

FIG. 13. Strength of the attractive force between two neighbor spheres f (in units of $\epsilon_f E_0^2 a^2$) vs d. (a) $\kappa=2$, (b) $\kappa=5$, and (c) $\kappa=10$. Both the results from the pair-force formula and the dipole model are also included.
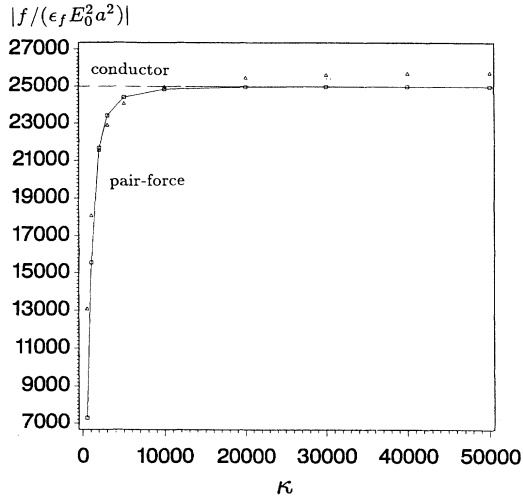
$|f/(\epsilon_f E_0^2 a^2)|$

FIG. 14. Strength of the attractive force between two neighbor spheres f (in units of $\epsilon_f E_0^2 a^2$) vs κ at $d = 2.00002a$. − − −, results of the conductor model; $\triangle$ points, FEA results; $\square$ points, results of the pair-force formula, Eq. (4.2).

$\kappa = 10$, the dipole model underestimates the strength of chain by a factor of 6.

Figures 13(a)–13(c) also indicate that the attractive force between two touching dielectric spheres is finite. A previous calculation based on multipole expansion finds this force to be infinite, which is unphysical because two touching dielectric spheres in an electric field do not collapse [14]. The pair attractive force will become infinite only if $\kappa \to \infty$.

As shown in Fig. 13(c), at $\kappa = 10$ and $d = 2a$, the FEA result of the pair force is about six times as strong as the dipolar result. The FEA calculation of a tetragonal lattice structure at $d = 2a$ and $w = 3.236a$ finds this ratio to be about 9 [17]. Though the tetragonal lattice is not the ideal structure of ER fluids [7], the above results indicate that a lattice structure will further enhance the pair attractive force

To have an empirical fit to the FEA results, we introduce the following formula, which gives a good approximation to the neighbor-pair attractive force,

$$f_{\text{pair}} = -\epsilon_f E_0^2 a^2 \frac{a^4 \beta^2 (6d - 4a)}{d^4 (d - 2a\beta^{(1-\beta)/2})} \ . \tag{4.2}$$

Results from Eq. (4.2) have been plotted in Figs. 13(a)–13(c). They are better than the results from the dipole model.

In Fig. 14 we plot this attractive force as a function of κ at $2.00002a$. The horizontal dashed line is the result of the conductor model, Eq. (3.11). For a comparison, we also plot the result from Eq. (4.2) in Fig. 14. It is clear that the new pair force formula matches the FEA result very well.

Our formula seems to cover the whole range of interest. If β is small or d is big, Eq. (4.2) recovers the dipolar result. If we take $\beta = 1$ for the conductor spheres, then Eq. (4.2) is identical to Eq. (3.12), the leading term

of the conductor sphere model.

When the spheres are in contact, $d = 2a$, Eq. (4.2) gives the neighbor attractive force

$$f_{\text{pair}} = -\frac{\epsilon_f E_0^2 a^2 \beta^2}{4(1 - \beta^{(1-\beta)/2})} \ . \tag{4.3}$$

If $\kappa \gg 1$, then $\beta \to 1$, we can approximate

$$\beta^{(1-\beta)/2} = \exp\left[\frac{1-\beta}{2} \ln[1 - (1-\beta)] \right]$$

$$\approx 1 - (1-\beta)^2/2 \ . \tag{4.4}$$

Thus we have the leading term

$$f_{\text{pair}} \approx -\tfrac{1}{18} \epsilon_f E_0^2 a^2 (\kappa - 1)^2 \ . \tag{4.5}$$

It is very interesting to note that Anderson's result estimates this force as [15]

$$-0.52 \epsilon_f E_0^2 a^2 \kappa^2 / (4\pi) = -0.04138 \epsilon_f E_0^2 a^2 \kappa^2 \ . \tag{4.6}$$

Since $\kappa \gg 1$, both results are proportional to κ^2. However, our force is slightly stronger than Anderson's result in the above limit.

We also note that the pair force of our FEA result in Eq. (4.3) is proportional to E_0^2, while the conduction model [20] has the leading term of the pair force proportional to E_0. The conduction model assumes that the conductivity of the base liquid is a function of the local field which, in turn, limits the upper value of the local field. Our present FEA calculation does not place any cap on the local field. Therefore, the above difference should be understandable.

V. CONCLUSIONS

We have solved the Laplace equation in closed form for an infinite chain of dielectric particles in a dielectric fluid and compared the electric field, energy, and pair attractive force with the dipole model, conductor sphere model, and other published results.

When $\kappa = \epsilon_p / \epsilon_f \leq 10$, the dipole model seems to give a good approximation for the energy, even if the particles get very close. Therefore, in calculating the energy, the dipole model can be used as an approximation for a rather wide range of κ.

However, the dipolar model underestimates the pair attractive force when the particles are in contact or very close. For example, at $\kappa = 2$ and $d = 2a$, the attractive pair force from the dipole model is about 70% of the FEA result, while at $\kappa = 10$ and $d = 2a$, the result from the dipole model is only about 10% of the FEA result. The bigger κ is, the poorer is the dipolar model. However, when κ is finite, the attractive force is finite. When two dielectric particles are in contact, their attractive force does not go into infinite.

The conductor model is a good approximation when the two particles are very close and $\kappa \geq 1000$. Otherwise, the conductor model overestimates the pair attractive force.

Based on our FEA calculation, we proposed Eq. (4.2) to calculate the neighbor pair attractive force. When $\kappa \gg 1$ and two spheres get very close, Eq. (4.2) is the same as the leading term from the conductor model. When κ is not too big, Eq. (4.2) is also approaching to the result obtained from the dipole model. When the chain is close packed and κ is large, Eq. (4.2) also gives f_{pair} proportional to κ^2, consistent with Anderson's result. A comparison of Eq. (4.2) with the FEA result suggests that this formula may cover the whole range of interest.

ACKNOWLEDGMENT

[1] For example, see *Electroheological Fluids,* edited by R. Tao and G. D. Roy (World Scientific, Singapore, 1994).

[2] W. M. Winslow, J. Appl. Phys. **20**, 1137 (1949).

[3] R. Tao, J. T. Woestman, and N. K. Jaggi, Appl. Phys. Lett. **55**, 1844 (1989).

[4] H. Block and J. P. Kelly, US Patent No. 4, 687, 589 (1987).

[5] F. E. Filisko and W. E. Armstrong, US Patent No. 4, 744, 914 (1988).

[6] T. C. Halsey and W. Toor, Phys. Rev. Lett. **65**, 2820 (1990).

[7] R. Tao and J. M. Sun, Phys. Rev. Lett. **67**, 398 (1991).

[8] R. Tao, Phys. Rev. E **47**, 423 (1993).

[9] T. J. Chen, R. N. Zitter, and R. Tao, Phys. Rev. Lett. **68**, 2555 (1992).

[10] R. Tao and Q. Jiang, Phys. Rev. Lett. **73**, 205 (1994).

[11] D. J. Klingenberg, F. van Swol, and C. F. Zukoski, J. Chem. Phys. **91**, 7888 (1989).

[12] D. J. Klingenberg, F. van Swol, and C. F. Zukoski, J. Chem. Phys. **94**, 6160 (1991).

[13] J. R. Melrose and D. M. Heyes, J. Chem. Phys. **98**, 5873 (1993).

[14] Y. Chen, A. F. Sprecher, and H. Conrad, J. Appl. Phys. **70**, 6796 (1991).

[15] R. A. Anderson, Langmuir **10**, 2917 (1994).

[16] L .C. Davis, Appl. Phys. Lett. **60**, 319 (1992).

[17] L. C. Davis, J. Appl. Phys. **72**, 1334 (1992).

[18] H. J. H. Clerec and G. Bossis, Phys. Rev. E **48**, 2721 (1993).

[19] R. Friedberg and Y. Yu, Phys. Rev. B **46**, 6582 (1992).

[20] N. Felici, J. F. Foulc, and P. Atten, in *Electroheological Fluids* (Ref. [1]), p. 139.

[21] L. D. Landau and E. M. Lifshitz, *Electrodynamics of Continuous Medium* (Pergamon, Oxford, 1983), pp. 36–91.

[22] L. C. Davis, Phys. Rev. A **46**, R719 (1992).